Peer-reviewed version available at Frontiers in Physics 2020, 8, 276; doi:10.3389/fphy.2020.00276

Gaussian doubling times and reproduction factors of the COVID-19 pandemic disease

M. Kröger[1,*], R. Schlickeiser[2,3,**]
1 Polymer Physics, Department of Materials, ETH Zurich, Zurich CH-8093, Switzerland, ORCID 0000-0003-1402-6714
2 Institut für Theoretische Physik, Lehrstuhl IV: Weltraum- und Astrophysik, Ruhr-Universität Bochum, D-44780 Bochum, Germany, ORCID 0000-0003-3171-5079
3 Institut für Theoretische Physik und Astrophysik, Christian-Albrechts-Universität zu Kiel, Leibnizstr. 15, D-24118 Kiel, Germany
(Dated: May 12, 2020)

The Gauss model for the time evolution of the first corona pandemic wave rendered useful in the estimation of peak times, amount of required equipment, and the forecasting of fade out times. At the same time it is probably the simplest analytically tractable model that allows to quantitatively forecast the time evolution of infections and fatalities during a pandemic wave. In light of the various descriptors such as doubling times and reproduction factors currently in use to judge about lock-downs and other measures that aim to prevent spreading of the virus, we hereby provide both exact, and simple approximate relationships between the two relevant parameters of the Gauss model (peak time and width), and the transient behavior of two versions of doubling times, and three variants of reproduction factors including basic reproduction numbers.

Keywords: coronavirus; statistical analysis; extrapolation; parameter estimation; pandemic spreading

I. INTRODUCTION

Recently[1] (hereafter referred to as SSSK), we demonstrated that the proposed[2–4] Gaussian time evolution for the daily number of cases (deaths, or alternatively infections) at time t

$$c(t) = c_{\max}\, e^{-\left(\frac{t-t_{\max}}{w}\right)^2} \tag{1}$$

provides a quantitatively correct description for the monitored rates in 25 different countries. Here, $c_{\max}$ is the maximum number of daily cases at peak time $t_{\max}$, and w a characteristic duration. The Gauss model (GM) is capable to reproduce reasonably well the monitored time evolution of the Covid-19 disease, and even more important to make realistic predictions for the future evolution of the first wave in different countries.

Values for the parameters of the GM had been extracted by fitting the natural logarithm of the monitored rates with

$$\begin{aligned}\ln c(t) &= \ln c_{\max} - \left(\frac{t-t_{\max}}{w}\right)^2 \\ &= \ln c_{\max} - \frac{t_{\max}^2}{w^2} + \frac{2t_{\max}t}{w^2} - \frac{t^2}{w^2},\end{aligned} \tag{2}$$

which is a polynomial of second order in t, to derive the best fit values and their confidence errors of the three parameters $c_{\max}$, w and $t_{\max}$. These parameters are are country-specific and reflect the regional differences in treatment, geographical, political, socioeconomic situations, available equipment etc.. If this fitting and parameter determination is done during the early stage of the pandemic wave, the GM makes predictions for the later time evolution of the wave.

The starting time of the outbreak, t_0 can be defined by the first occurrence of a case, $c(t_0) = 1$, and is thus known from the parameters of the Gaussian. Inverting $c(t_0) = 1$ readily yields $\ln(c_{\max}) = (t_0 - t_{\max})^2/w^2$, or

$$t_0 = t_{\max} - w\sqrt{\ln c_{\max}} \tag{3}$$

To simplify notation, besides absolute time t we introduce two more times. First, the time relative to the peak time, denoted by

$$\Delta = t - t_{\max} \tag{4}$$

so that negative (positive) Δ correspond to times before (after) the peak time. Second, the dimensionless time $x = -\Delta/w$. As time unit we choose days throughout, so that $\Delta = +2$ corresponds to two days after peak time, and w is also given in units of days, while c is a dimensionless number of cases, usually renamed as d or i if we specialize to deaths or infections. The three parameters of the GM are related, but not identical for deaths and infections, as discussed earlier[1].

The related (to equation (3)) starting time

$$\Delta_0 = t_0 - t_{\max} = -wx_0 = -w\sqrt{\ln c_{\max}} \tag{5}$$

is negative, $x_0 = \sqrt{\ln c_{\max}}$ is positive, and $|\Delta_0|$ is the number of days between outbreak and climax of the first pandemic wave. All properties derived for the GM must therefore depend on w, $c_{\max}$, and x or alternatively Δ, where $\Delta \in [\Delta_0, \infty]$.

Often monitored data are reported in terms of doubling times and effective reproduction factors. These are also important indicators for the future temporal evolution of the disease, especially if no functional form for the case temporal evolution, such as the GM (2), is adopted.

* mk@mat.etz.ch, rsch@tp4.rub.de

However, there are differently defined doubling times as well as reproduction factors in use. It is the purpose of this manuscript to discuss in detail the properties of differently defined doubling times and the differently defined reproduction factors, their mutual relations to each other, and their temporal behavior for the GM.

II. DAILY INSTANTANEOUS DOUBLING TIME

As before[2] we consider the relative change of the daily number of cases for the GM

$$p(t) = \frac{c'(t)}{c(t)} = [\ln c(t)]' = -\frac{2\Delta}{w^2} = \frac{2x}{w}, \tag{6}$$

where the prime denotes a derivative with respect to time t, $c'(t) = dc(t)/dt$. The monitored data are often given in terms of the instantaneous doubling time d of the corresponding exponential functions at any time for the daily number of cases

$$c_a(t) \propto e^{\frac{t \ln 2}{d}} = 2^{t/d}, \tag{7}$$

with the obvious properties $c_a(t+d) = 2c_a(t)$. With these corresponding exponential functions we obtain for the relative changes in the daily rate

$$p(t) = [\ln c_a(t)]' = \frac{\ln 2}{d}. \tag{8}$$

Equating the two results (6) and (8) leads to the time-dependent differential Gaussian doubling time

$$d(t) = -\frac{A}{\Delta}, \qquad A = w^2 \ln\sqrt{2} = 0.35w^2. \tag{9}$$

Apart from the changed notation these differential Gaussian doubling times agree with the earlier derived equation (5) in ref.[2]. The differential doubling time is positive for times earlier than the peak time, $\Delta < 0$, monotonically increases in the course of time until it diverges as it approaches $\Delta = 0$. For later times $\Delta > 0$ the doubling time is formally negatively valued, but corresponds to positively valued half-lifes approaching 0 for $\Delta \to \infty$. Because of the divergence at $\Delta = 0$ and its negative value for $\Delta > 0$ daily doubling times are of limited use only before the peak time of the outburst; instead in the public discussion often cumulative doubling times are preferred, which we discuss in the next subsection.

Apart from the time Δ relative to the peak time the daily instantaneous doubling time (9) is determined by the width w of the Gaussian time evolution function (1). Fig. 1 displays the distribution of widths w determined by the best fit of the GM to the death rates in 67 countries, indicating that $w \in [12, 34]$ with a mean value of 18.96.

We emphasize that at early times t of the time evolution, characterized by $t_0 \le t \ll t_{\max}$, or equivalently, $\Delta_0 \le \Delta \ll 0$, the Gaussian time evolution function (1) approaches an exponential distribution because the exponent $-(t - t_{\max})^2 \approx -t_{\max}^2 + 2t_{\max}t$ becomes linear in t, and thus also linear in Δ. At such early times the time relative to the peak time (4) is Δ_0, so that the differential Gaussian doubling time (8) approaches the constant

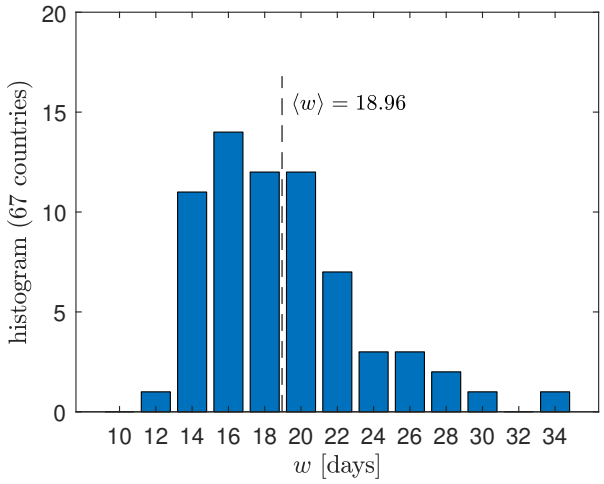

FIG. 1. Distribution of widths w obtained by the best fit of the GM to the death rates in 67 different countries.

$$d_0 \simeq d(t_0) = -\frac{A}{\Delta_0} = \frac{0.35w^2}{t_{\max} - t_0}, \tag{10}$$

characterizing the initial, exponential growth.

III. CUMULATIVE DOUBLING TIME

Instead of defining doubling times with daily number of cases one may also define them with the cumulative case rate.

From equation (1) with (4) one has for the corresponding cumulative number of cases at time t

$$C(t) = \int_{-\infty}^{t} ds\, c(s) = \frac{C_{\rm tot}}{2}\left[1 + \mathrm{erf}\,(\Delta/w)\right], \tag{11}$$

respectively, in terms of the error function, where

$$C_{\rm tot} = \sqrt{\pi}\, c_{\max} w \tag{12}$$

denotes the total number of cases. Such values for fatalities, $D_{\rm tot}$, and infections, $I_{\rm tot}$ relevant for the first pandemic wave of the Sars-Cov-2 virus had been obtained in SSSK.

With the cumulative numbers (11) we find for the respective relative change

$$P(t) = [\ln C(t)]' = \frac{C'(t)}{C(t)} = \frac{c(t)}{C(t)}. \tag{13}$$

Equating these results again with equation (8) for the corresponding exponential function? leads to the time-dependent cumulative Gaussian doubling times

$$D(t) = \frac{C(t)\ln 2}{c(t)} = \chi w e^{(\Delta/w)^2}[1 + \mathrm{erf}\,(\Delta/w)], \tag{14}$$

where $\chi = \sqrt{\pi}\ln(\sqrt{2}) \simeq 0.614$ abbreviates the numerical prefactor.

Using the identities $1+\mathrm{erf}(x) = 1-\mathrm{erf}(-x) = \mathrm{erfc}(-x)$ in terms of the complimentary error function, we express equation (14) as

$$D(t) = \chi w F\left(-\frac{\Delta}{w}\right) \tag{15}$$

with the function

$$F(x) = e^{x^2}\,\mathrm{erfc}\,(x) \tag{16}$$

As opposed to doubling times calculated from daily rates, doubling times derived from cumulative numbers are strictly positive, monotonically increase in the course of time, but never diverge, and remain finite at $\Delta = 0$. Because $x = -\Delta/w$, the argument x of $F(x)$ is positive before, and negative after the peak time.

In Appendix A we investigate the properties of the function $F(x)$ and its approximations. It is convenient to consider times t before and after the peak time $t_{\max}$, i.e. negative and positive Δ. We consider each in turn.

A. Before peak time $\Delta < 0$

With the approximation (A7) we obtain for the cumulative doubling time (15) at times $t \le t_{\max}$

$$D^{\mathrm{before}}(t) \simeq \frac{(\chi/3)w^2}{w + 0.5|\Delta|}\left[1 + \frac{2w^2}{(w+0.5|\Delta|)^2}\right] \tag{17}$$

where $\Delta = t - t_{\max}$ is negative, and $\chi/3 \simeq 0.205$. $D^{\mathrm{before}}(t)$ continuously increases with time until it reaches $D^{\max}$ (21) at peak time.

At early times of the time evolution $t \ll t_{\max}$, not only d, but also the cumulative Gaussian doubling time (15) or (17) approaches the constant

$$D_0 = D^{\mathrm{before}}(t_0) \tag{18}$$

reflecting again the result that at early times the Gaussian time distribution function (1)approaches an exponential distribution function with the constant doubling time (10), so that also the cumulative distribution function initially displays an exponential behavior.

The ratio of the two, differential (10) and cumulative (18), limits is given by

$$\frac{D_0}{d_0} = \frac{\sqrt{\pi}F(x_0)}{x_0}, \qquad x_0 = \frac{t_{\max} - t_0}{w} \tag{19}$$

with F from eq (16).

B. After peak time, $\Delta > 0$

Here we use the property (A3) and the approximation (A7) to obtain formally for the cumulative doubling time

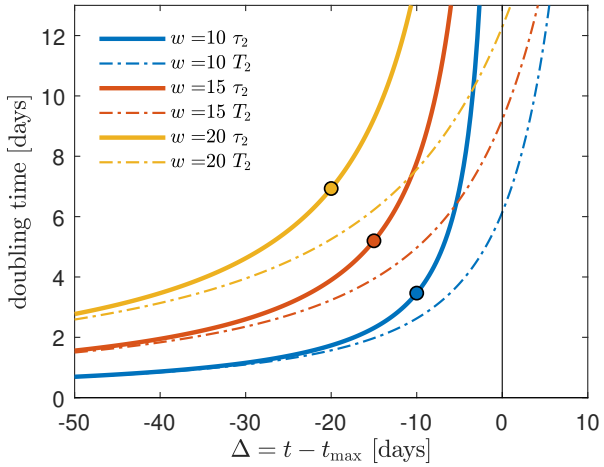

FIG. 2. Comparison of the daily instantaneous (d) and cumulative (D) doubling times as a function of the time Δ relative to the peak time for three values of the Gaussian width $w = 10, 15, 20$. The circles mark Δ_0 for $c_{\max} = 1$ (see equation (5)): the GM should not be used at times smaller than Δ_0.

(15)

$$D^{\mathrm{after}}(t) = \chi w\left[2e^{(\Delta/w)^2} - F\left(\Delta/w\right)\right] \simeq 2\chi w e^{(\Delta/w)^2} - D^{\mathrm{before}}(t) \tag{20}$$

with $2\chi \simeq 1.229$, and where we can make use of $D^{\mathrm{before}}(t)$ from (17) because it was written for this purpose in terms of $|\Delta|$.

However, this Gaussian cumulative doubling time $D^{\mathrm{after}}(t)$ for times $t > t_{\max}$ is only a formal indicator for the decreasing slope of the cumulative rate $C(t)$. As the cumulative rate (11) indicates, at the peak times $t_{\max}$ it has the value $C(t_{\max}) = C_{\mathrm{tot}}/2$, so that for any times larger than $t_{\max}$ the cumulative rates can no longer double. This implies that only the maximal cumulative doubling time

$$D^{\max} = D(t_{\max}) = \chi w \simeq 0.614w \tag{21}$$

has a real physical meaning.

In Fig. 2 we calculate the Gaussian daily instantaneous and cumulative doubling times as a function of the time Δ relative to the peak time for three values of the Gaussian width $w = 10, 15, 20$. It can be seen that at times below the peak time $\Delta < 0$ the two doubling times have a similar behavior. As $\Delta \to 0$ the instantaneous doubling times becomes infinitely large, whereas the cumulative doubling times approaches large but finite values. However, as noted before, for times $\Delta > 0$ the Gaussian cumulative doubling time $D^{\mathrm{after}}(t)$ is only a formal indicator for the decreasing slope of the cumulative rate $C(t)$ that can no longer double at any times larger than $t_{\max}$.

Nevertheless, cumulative doubling times are issued by health agencies such as the Robert-Koch-Institut to the

public also at times after the peak time: they highly confuse the ordinary public people, as they suggest by their name that the cumulative case rate can still double beyond its 50 percent value, although this is no longer possible. Instead one should refer to the effective reproduction factor at this stage of the wave time evolution, which we discuss next.

IV. BASIC REPRODUCTION NUMBER R_0 AND EFFECTIVE REPRODUCTION FACTOR $R(t)$

In epidemiology, the basic reproduction number R_0 (sometimes called basic reproductive ratio, or incorrectly basic reproductive rate), of an infection can be thought of as the expected number of cases directly generated by one case in a population where all individuals are susceptible to infection[10,11]. The definition describes the state where no other individuals are infected or immunized (naturally or through vaccination). Some definitions, such as that of the Australian Department of Health, add absence of any deliberate intervention in disease transmission.

The basic reproduction number R_0 is not to be confused with the effective, time-dependent reproduction number $R(t)$, which is the number of cases generated in the current state of a population, which does not have to be the uninfected state. By definition, R_0 cannot be modified through vaccination campaigns. Also, it is important to note that R_0 is a dimensionless number and not a rate, which would have units of time like doubling time[10,11]. Still, the basic reproduction number R_0 will be seen to correspond to $R(t)$ evaluated at time t_0.

The definition of the effective reproduction factor $R(t)$ according to[7,8] is

$$c(t) = R(t) \sum_{s=-\infty}^{t} W(t-s)c(s) \tag{22}$$

where $c(t)$ is the number of daily cases (deaths or infections, usually the reproduction factor is obtained from the reported number of daily infections) at time t and $W(s)$ denotes the serial interval distribution. The discrete sum in (22) starts from zero rather than unity as in Ref.[7,8], because $W(0) = 0$, and because we are here interested in the continuous generalization of (22).

Written in terms of integrals, equation (22) corresponds to[9]

$$R(t) = \frac{c(t)}{\int_0^\infty W(s)c(t-s)\,ds} \tag{23}$$

while the serial interval distribution $W(s)$ has to be properly normalized to unity, i.e.

$$\int_0^\infty dsW(s) = 1 \tag{24}$$

This normalization is required in order to ensure according to equation (23) that a constant stationary $c(t)$ implies $R(t) = 1$. Note that in ref.[8] they wrote $E[c(t)]$ instead of $c(t)$ on the left hand side of equation (22), where $E[]$ stands for an expectation value. Here we can assume that $c(t)$ is known by the GM, c.f. equation (1).

In the following we investigate two different choices of the serial interval distribution, evaluated for the GM: (i) as in previous studies[7,8] the gamma distribution, and (ii) the analytically simpler box-shaped serial interval distribution. We consider each in turn.

A. Gamma serial interval distribution

Here the serial interval distribution $W(s)$ is taken to be the gamma distribution[5]

$$W(s) = \frac{\beta^\alpha s^{\alpha-1} e^{-\beta s}}{\Gamma(\alpha)} \tag{25}$$

with the shape parameters $\alpha = 2.785$ and $\beta = \alpha/6.5$ that seem to represent the distribution used in Ref.[7]. They used another convention, but mentioned the mean value $\langle s\rangle = 6.5$ and provided an excel file. The mean value of this distribution (25) is

$$\langle s\rangle = \int_1^\infty sW(s)\,ds = \frac{\alpha}{\beta} \tag{26}$$

For the specified parameters the distribution (25) is very well approximated (absolute error less than 0.006) by the slightly more convenient, and again properly normalized distribution

$$W(s) = \frac{b^3}{2} s^2 e^{-bs}, \tag{27}$$

yielding as mean value $\langle s\rangle = 3/b$. We adopt $b = 4/9 = 0.444$, leading to the mean $\langle s\rangle = 27/4 = 6.75$ days, very close to the earlier chosen mean[7] $\langle s\rangle = 6.5$ days. In Fig. 3 we compare the approximation (27) with the discrete distribution used in Ref.[7] (black circles) during all their calculations.

1. *Reproduction factor $R(t)$*

Here we use the known $c(t) = c_{\max} \exp[-(\Delta/w)^2]$ for the GM (1). As for the doubling times, $R(t)$ does not depend on the magnitude $c_{\max}$ and absolute time t, but can be expressed in terms of the relative time $\Delta = t - t_{\max}$ and w. With $c(t-s) \sim \exp[-(\Delta-s)^2/w^2]$ and with $W(s)$ from equation (27) we can thus proceed and calculate $R(t)$ analytically as

$$R(t) = \frac{2}{b^3 J(t)} \tag{28}$$

involving the time-dependent integral

$$J(t) = \int_0^\infty ds\, s^2 e^{-q_1 s - q_2 s^2}, \tag{29}$$

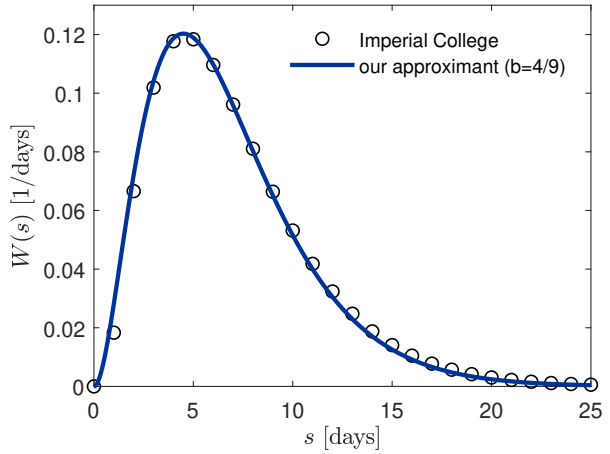

FIG. 3. Comparison of $W(s)$ employed in[7,8] (black circles) and the approximant (27).

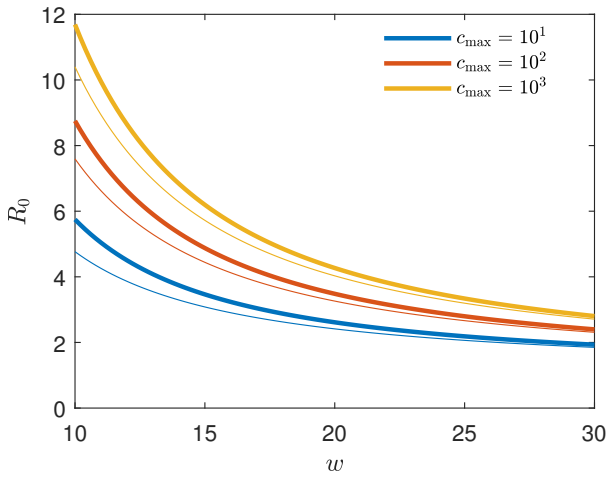

FIG. 4. Basic reproduction number $R_0 = R(t_0)$ for the GM as function of peak width w for several peak heights $c_{\max}$ (thick solid lines). For comparison, the thin lines show the approximant (34). The exact R_0 is given by eq (33) evaluated at $x = x_0 = \sqrt{\ln c_{\max}}$.

where $q_2 = w^{-2}$ and $q_1(t) = b - 2\Delta/w^2$. To this end it turns out convenient to switch to dimensionless times. We had already introduced x, we now introduce a characteristic x_c

$$x_c = -\frac{bw}{2}, \tag{30}$$

and the dimensionless, again time-dependent distance X between x and x_c via

$$X(t) = x - x_c = \frac{bw}{2} - \frac{\Delta}{w} = \frac{wq_1}{2}. \tag{31}$$

As shown in Appendix B, the integral (29) can be evaluated analytically to yield

$$J(t) = \frac{\sqrt{\pi}w^3}{4}\frac{d}{dX}[XF(X)]$$

$$= \frac{w^3}{4}\left[(1+2X^2)\sqrt{\pi}F(X) - 2X\right] \tag{32}$$

with the function F given by equation (16). Consequently, the effective reproduction factor (28) becomes (Fig. 5)

$$R(t) = \frac{-1}{x_c^3\sqrt{\pi}\frac{d}{dX}[XF(X)]}$$

$$= \frac{1}{x_c^3\left\{2(x-x_c) - [1+2(x-x_c)^2]\sqrt{\pi}F(x-x_c)\right\}} \tag{33}$$

in terms of x, and the negatively valued x_c, where we recall that $x = (t_{\max} - t)/w = -\Delta/w$ carries the dependency on time t. The effective reproduction factor approaches the basic reproduction number R_0 at small times and assumes the important value $R(t) = 1$ roughly 4 days after peak time, at $\Delta \approx 4$, as Fig. 5 indicates. It is not difficult to show that this Δ asymptotically approaches $2/b = 9/2 = 4.5$ days for large w (Appendix D 1).

2. *Base reproduction number R_0*

While the basic reproduction number R_0 for the GM can be read off from eq (33) upon replacing x by $x_0 = \sqrt{\ln c_{\max}}$ (shown in Fig. 4), it is insightful to make the connection between R_0 and the early doubling time $d_0 = (\ln\sqrt{2})w/x_0$, according to equation (10). As the Gaussian time distribution is exponential at early times, in the vicinity of $t \simeq t_0$, we can insert the exponential growth (7) into definition (23) with the gamma-shaped serial distribution $W(s)$. This yields a time-independent constant effective reproduction factor

$$R_0 = R(t_0) \approx \frac{2}{b^3\int_0^\infty ds\, s^2 \exp[-(b + \frac{\ln 2}{d_0})s]}$$

$$= \left(1 + \frac{\ln 2}{bd_0}\right)^3 = \left(1 - \frac{x_0}{x_c}\right)^3 \tag{34}$$

where $b = 4/9$, and where we have also mentioned its appearance in terms of dimensionless x_0 and x_c. Since d_0 is positive, the exponential effective reproduction factor at time t_0 (34) is greater than unity, and provides an approximation for the exact one (Fig. 4). It is worthwhile to mention that the same result is obtained without assuming a purely exponential growth, but instead starting from eq (33), and assuming $x_0 \gg x_c + 1$ (for a proof see Appendix C 1). For a model with purely exponential growth characterized by a single doubling time d_0, eq (34) provides the exact relationship between doubling time and basic reproduction number, and $R(t) = R_0$.

Adopting $b = 4/9$ and $w = 20$ and thus $x_c = -40/9$ according to eq (30), provides for the number (34)

$$R_0^{w=20} = \left(1 + 0.225\sqrt{\ln c_{\max}}\right)^3, \tag{35}$$

yielding the estimates 4.77, 4.03, and 3.26 for $c_{\max} = 10^4$, 10^3, and 10^2, respectively, close to the exact values given by $R(t_0)$ from eq (33). The values of Δ_0 and R_0 for different values of the width w and $c_{\max} = 1$ are marked by circles in Fig. 5.

B. Box-shaped interval distribution

With this section we address the question on how relevant it is to take into account the correct shape of serial interval distribution when calculating $R(t)$ via equation (23).

If we consider $W(s)$ to be approximated by a constant independent on s on the interval $s \in [0, s_{\max}]$, and zero otherwise, the requirement of its proper normalization (24) and mean value $\langle s \rangle = 6.5$ yields

$$W(s) = \frac{\Theta(s; 0, s_{\max})}{s_{\max}}, \qquad s_{\max} = 2\langle s \rangle = 13 \tag{36}$$

with the two-sided Heaviside $\Theta(x, A, B) = 1$ for $A \le x \le B$ and $\Theta(x) = 0$ otherwise.

1. Reproduction factor $R(t)$

With the Gaussian evolution (1) and the box-shaped serial interval distribution (36) inserted we obtain with the help of equation (23)

$$\begin{aligned} R(t) &= \frac{s_{\max}}{\int_0^{s_{\max}} \exp[(2\Delta - s)s/w^2]\, ds} \\ &= \frac{2s_{\max}/w}{\sqrt{\pi} e^{(\frac{\Delta}{w})^2} \left[\mathrm{erf}\,(\Delta/w) - \mathrm{erf}\,([\Delta - s_{\max}]/w)\right]} \\ &= \frac{26/w}{\sqrt{\pi}\left[e^{\frac{26(\Delta-6.5)}{w^2}} F\left(\frac{\Delta-13}{w}\right) - F\left(\frac{\Delta}{w}\right)\right]} \end{aligned} \tag{37}$$

plotted in Fig. 5. As is visible, the box-shaped $W(s)$ can serve as a good approximation as long as w is sufficiently large, and Δ not too small. It crosses the $R = 1$ line roughly 4 days after peak time, and shares this feature with the case of the gamma-shaped serial distribution. Starting from $R(t) = 1$ with $R(t)$ from eq (37), the exact asymptotic value is $t = t_{\max} + (s_{\max}/3)$ days (proof in Appendix D 2).

2. Base reproduction number R_0

The basic reproduction number is given by $R(t_0)$, which amounts to replacing Δ by Δ_0 in eq (37). As before, it is useful to consider a regime of exponential growth to come up with a simple approximant for R_0, now using a box-shaped $W(s)$. Inserting the exponential time evolution (7) with constant d_0 and the box-shaped serial interval distribution (36) into equation (23) we obtain the time-independent constant effective box reproduction factor that serves an approximant for R_0,

$$R_0 = R(t_0) \approx \frac{s_{\max} \ln 2/d_0}{1 - e^{-s_{\max} \ln 2/d_0}} \tag{38}$$

which is always greater than unity for positive d_0. Since $s_{\max} \ln 2 \approx 9$ days, we thus have

$$R_0 \approx 9/d_0 \tag{39}$$

as long as $d_0 < 9$ days, which is the usual scenario (Fig. 2). As already mentioned, the box-shaped serial interval distribution is better not used to estimate R_0. It significantly underestimates the R_0 obtained with the gamma serial distribution.

C. Robert Koch institute (RKI)

The RKI estimates an effective reproduction factor from the daily measured number $i(t)$ of people that have been recognized to be infected as follows

$$R(t) = \frac{\int_{t-4}^{t} ds\, i(s)}{\int_{t-8}^{t-4} ds\, i(s)} \tag{40}$$

Here we again use the continuous version. Because measured data is not available for the future, and not sufficiently reliable if collected within the time frame of a few days, the RKI estimates $R(t)$ for a time t that lies one 8 days the past. A connection between (40) and the true effective reproduction number is based on the assumption that the true number of cases is proportional to the measured ones, at any time.

1. Reproduction factor $R(t)$

Using the GM instead of measured numbers for $i(t)$, and thus the estimated true number of cases (deaths or infections) in eq (40) yields

$$R(t) = \frac{\mathrm{erf}[\Delta/w] - \mathrm{erf}[(\Delta - 4)/w]}{\mathrm{erf}[(\Delta - 4)/w] - \mathrm{erf}[(\Delta - 8)/w]} \tag{41}$$

shown in Fig. 5. With (41) at hand one can predict the RKI version of $R(t)$ at all times during the first wave of a pandemy. A time of interest is when R drops below unity. Equation (41) readily yields for $\Delta = 4$, with $\mathrm{erf}(0) = 0$,

$$R(t_{\max} + 4) = -\frac{\mathrm{erf}(4/w)}{\mathrm{erf}(-4/w)} = 1, \tag{42}$$

in agreement with Fig. 5. It is this feature of the RKI, shared with the $R(t)$ for the gamma serial distribution, that may have given rise to the choice of the interval length of 4 days in its definition. Figure 6 shows, for typical values between $w = 15$ and $w = 20$ days, how the $R(t)$ calculated via the box-shaped $W(s)$, and even more the RKI value, overestimate the $R(t)$ at times beyond peak time.

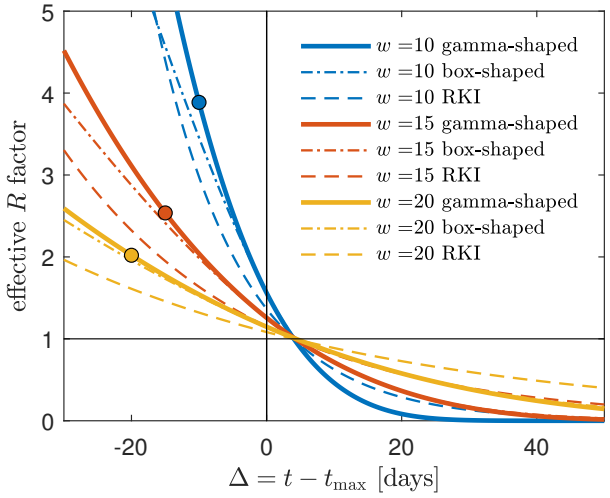

FIG. 5. Gamma-shaped $R(t)$ (eq 33) compared with the approximate $R(t)$ (red, dashed), eq (38), using a box-shaped serial interval distribution $W(s)$, and the RKI formula (41). Cases shown are $w = 10$, $w = 15$, and $w = 20$. Deviations are most pronounced and significant for the smallest $w = 10$. The $R(t)$ curves terminate at $t = t_0$ corresponding to $\Delta = \Delta_0$ (see equation (5)). The circles mark Δ_0 for $c_{\max} = 1$.

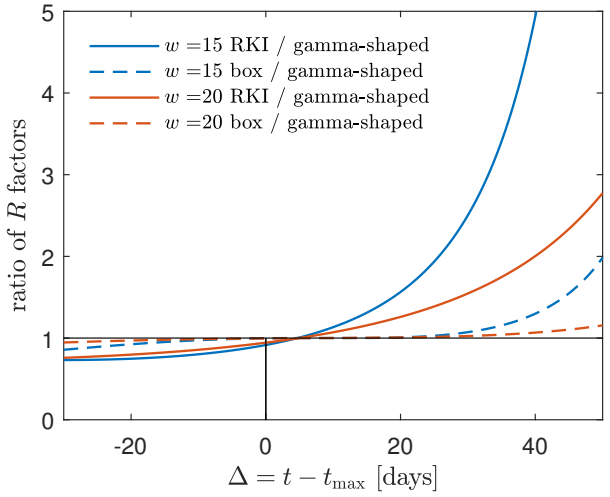

FIG. 6. The $R(t)$ factors obtained using (i) the box-shaped $W(s)$ and (ii) the RKI formula greatly overestimate the $R(t)$ using a gamma-shaped serial interval distribution at times beyond the peak time. Alternative representation of the data already shown in Fig. 5. The mismatch increases with decreasing w. A typical w is in the range between 15 and 20 days for most countries[1], cf. Fig. 1.

2. *Base reproduction number R_0*

As in previous sections, we can read off the basic reproduction number R_0 upon inserting Δ_0 instead of Δ into the expression for $R(t)$, eq (41), and we can provide an approximate expression for R_0 upon considering purely exponential, initial growth. Following this route, inserting monoexponential $i(t) \propto 2^{t/d_0}$ into eq (40) yields

$$R_0 = R(t_0) \simeq \frac{2^{t/d_0} - 2^{(t-4)/d_0}}{2^{(t-4)/d_0} - 2^{(t-8)/d_0}} = 2^{4/d_0} \qquad (43)$$

While the two approximants (34) and (43) for basic reproduction numbers look different at first glance, they are quantitatively very similar: for $d_0 = 1$, for example, (34) evaluates to 16.77, while (43) equals 16.0. Likewise, for $d_0 = 2$ (34) evaluates to 5.64, while (43) equals 4.0. In the limit of $d_0 \to \infty$, both versions yield $R_0 = 1$. The RKI version generally underestimates R_0 as given by (34), but by no more than about 35%.

V. SUMMARY AND CONCLUSIONS

The Gauss model for the time evolution of the first corona pandemic wave rendered useful in the estimation of peak times, amount of required equipment, and the forecasting of fade out times. At the same time it is probably the simplest analytically tractable model that allows to quantitatively forecast the time evolution of infections and fatalities during a pandemic wave. For these descriptions and forecasts various descriptors such as doubling times and reproduction factors are currently used in order to judge about lock-downs and other non-pharmaceutical measures that aim to prevent spreading of the virus. As different definitions of doubling times and reproduction factors and numbers are used in the literature, we have provided in this manuscript both exact, and simple approximate relationships between the two relevant parameters of the Gauss model (peak time $t_{\max}$ and width w) as well as the transient behavior of two versions of doubling times, and three variants of reproduction factors $R(t)$ including basic reproduction numbers R_0.

Regarding doubling times we considered both, differential doubling times calculated from the daily number of cases, and cumulative doubling times calculated from the cumulative case rates. The former differential doubling time is positive for times earlier than the peak time, monotonically increases in the course of time until it diverges as it approaches the peak time. For later times after the peak time the differential doubling time is formally negatively valued, but corresponds to positively valued half-lifes. Because of the divergence at the peak time and its negative value beyond, differential doubling times are of limited use only before the peak time of the outburst; instead in the public discussion often cumulative doubling times are preferred.

As opposed to doubling times calculated from daily rates, doubling times derived from cumulative numbers of cases are strictly positive, monotonically increase in the course of time, but never diverge, and remain finite at and after the peak time. At times below the peak time the two doubling times have a similar behavior. However, the Gaussian cumulative doubling time for times after

the peak time is only a formal indicator for the decreasing slope of the cumulative rate of cases. The Gaussian cumulative rate at the peak time attains exactly 50 percent of its maximum value after infinite time, so that for any times larger than the peak time the cumulative rates can no longer double. This implies that only the maximal cumulative doubling time $0.614w$ has a real physical meaning.

Because of these two drawbacks of differential and cumulative doubling times in characterizing the time evolution of the corona wave after its peak time, health agencies such as the German Robert-Koch-Institute (RKI) instead refer to the effective reproduction factor of the disease $R(t)$ which is the number of cases infected in the current state of a population by a single individual infected person. As long as this factor remains smaller than unity the number of infections per day decreases with time. The effective reproduction factor is calculated from an integral involving the serial interval distribution $W(s)$ normalized to unity and the differential case time distribution. For the GM the latter is known analytically, so that we investigated three different effective Gaussian reproduction factors: (i) the first is calculated with a gamma-function type serial interval distribution, (ii) the second with a flat box-shaped serial interval distribution, and (iii) the third, referred to as RKI estimate, involves the ratio of two consecutive 4-day time intervals of the monitored daily cases.

All three discussed effective reproduction factors calculated with the GM decrease from the base reproduction number R_0 at the beginning of the pandemic wave to very small values at times much larger than the peak time. They all cross the critical value $R = 1$ about four days after the peak times. As the approximated RKI estimate for Germany still, many weeks after the peak times of the infection and death rates, occasionally indicates effective reproduction factors greater than unity, this has to be due to short intraday fluctuations of the rates. Such factors greater unity at late times after the peak time contradict the much smaller (below unity) effective reproduction factors from the GM, as we have demonstrated by Fig. 6. As the GM provides reasonable descriptions of the overall temporal evolution of the infection and death rates in Germany, we have to conclude that the RKI estimate of the effective reproduction factor overestimates the influence of short intraday fluctuations in the reported cases, and thus helps to misguide political decision makers and the public.

Appendix A: The function $F(x)$

The function $F(x)$ has the properties

$$F(0) = 1, \qquad F(x \to \infty) \to 0 \tag{A1}$$

and it fulfills the differential equation

$$\frac{dF(x)}{dx} = 2\left[xF(x) - \frac{1}{\sqrt{\pi}}\right]. \tag{A2}$$

$F(x)$ is monotonically decreasing with increasing x, as the right hand side of (A2) is negative for all x, and because its 2nd derivative is strictly positive.

Moreover, because of the property $\mathrm{erf}(-x) = -\mathrm{erf}(x)$, implying $\mathrm{erfc}(-x) = 2 - \mathrm{erfc}(x)$ we find for negative arguments

$$F(-x) = 2e^{x^2} - F(x) \tag{A3}$$

For positive values of $x \geq 0$ the rational approximation[5] of the function $F(x)$ is given by $F(x) = a_1 y - a_2 y^2 + a_3 y^3$ with $y = 1/(1 + qx)$, $q = 0.47047$, $a_1 = 0.3480242$, $a_2 = 0.0958798$, and $a_3 = 0.7478556$ (approximant I). Given the smallness of a_2 we use as even simpler approximation[6] for positive arguments

$$F(x) \simeq a_1 y + (1 - a_1)y^3 = a_1 y\left(1 + \frac{a_4}{a_1} y^2\right) \tag{A4}$$

with unchanged a_1, q, and $y = (1 + qx)^{-1}$, and where $a_4 = a_3 - a_2 = 1 - a_1 = 0.6519758$, and $a_4/a_1 \simeq 1.873$ (approximant II). It has been shown before (see Fig. 1 in ref.[6]) that the last approximation (A4) deviates at most by 5 percent from the earlier rational one by ref.[5]. We note that the rational approximation (A4) fulfils the properties (A1).

If we do not constrain the approximant to share coefficients with the one given in ref.[5], the approximant can be further improved (Fig. 7). An approximant with the correct asymptotic behavior must fulfill $\lim_{x\to\infty} xF(x) = 1/\sqrt{\pi}$, which can be inferred from eq (A2). This condition is not fulfilled for the above approximants, as it implies $q = \sqrt{\pi}a_1$. An ansatz parameterized by yet unknown a with correct both asymptotic behavior at $x \to \infty$ and correct value at $x = 0$ is

$$F(x) \approx y\frac{1 + 2ay^2}{1 + 2a}, \qquad y = \left(1 + \frac{\sqrt{\pi}x}{1 + 2a}\right)^{-1} \tag{A5}$$

We find $a = 8/5$ by minimizing the relative maximum error (shown as magenta curve in Fig. 7). Inserting this value for a, the approximant reads

$$F(x) \approx \frac{y}{21}(5 + 16y^2), \qquad y = \left(1 + \frac{5\sqrt{\pi}x}{21}\right)^{-1} \tag{A6}$$

A somewhat simpler approximant, sufficient for practical purposes, but with wrong asymptotic behavior, is (blue curve in Fig. 7)

$$F(x) \approx \frac{y}{3}\left(1 + 2y^2\right), \qquad y = (1 + 0.5x)^{-1} \tag{A7}$$

Appendix B: Derivation of equation (33)

We readily calculate (29) via

$$J = -\frac{\partial}{\partial q_2}\int_0^\infty ds\, e^{-q_1 s - q_2 s^2}$$

Preprints (www.preprints.org) | NOT PEER-REVIEWED | Posted: 13 May 2020 doi:10.20944/preprints202005.0219.v1

Peer-reviewed version available at *Frontiers in Physics* **2020**, *8*, 276; doi:10.3389/fphy.2020.00276

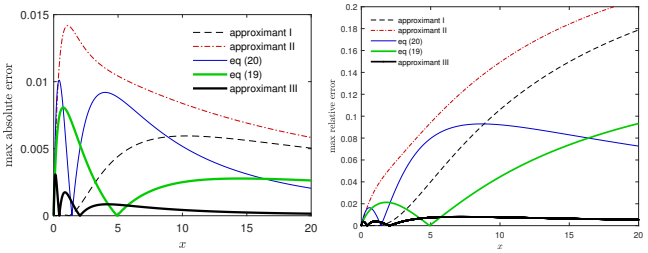

FIG. 7. Absolute and relative error of some approximants for $F(x)$ at $x \geq 0$. Approximant I from[5] involving the quadratic term with $a_2 = 0.0958798$, without quadratic term and unchanged $a_1 = 0.3480242$ and $q = 0.47047$ in $y = 1/(1+qx)$ (approximant II), without quadratic term and asymptotically correct behavior (eq A6), and with simpler coefficients (eq A7), asymptotically correct with quadratic term we find $a_1 = 0.656411$ and $a_2 = -0.770823$, $a_3 = 1 - a_1 + a_2$ and $q = \sqrt{\pi} a_1$ to be the parameters with the smallest maximum relative error (approximant III).

$$= -\frac{\sqrt{\pi}}{2}\frac{\partial}{\partial q_2}\left[q_2^{-1/2} e^{\frac{q_1^2}{4q_2}} \operatorname{erfc}\left(\frac{q_1}{2\sqrt{q_2}}\right)\right]$$
$$= -\frac{\sqrt{\pi}}{2}\frac{\partial}{\partial q_2}\left[q_2^{-1/2} F\left(\frac{q_1}{2\sqrt{q_2}}\right)\right] \qquad \text{(B1)}$$

in terms of the function (16). The property (A2) can then be used to provide

$$\frac{\partial}{\partial q_2} F\left(\frac{q_1}{2\sqrt{q_2}}\right) = \left[\frac{\partial}{\partial q_2}\left(\frac{q_1}{\sqrt{q_2}}\right)\right]\left[\frac{q_1}{2\sqrt{q_2}} F\left(\frac{q_1}{2\sqrt{q_2}}\right) - \frac{1}{\sqrt{\pi}}\right]$$
$$= -\frac{q_1}{2q_2^{3/2}}\left[\frac{q_1}{2\sqrt{q_2}} F\left(\frac{q_1}{2\sqrt{q_2}}\right) - \frac{1}{\sqrt{\pi}}\right]$$
$$= -\frac{q_1^2}{4q_2^2} F\left(\frac{q_1}{2\sqrt{q_2}}\right) + \frac{q_1}{2\sqrt{\pi} q_2^{3/2}} \qquad \text{(B2)}$$

With this result we obtain for the integral (B1)

$$J = \frac{\sqrt{\pi}}{2}\left[\frac{F}{2q_2^{3/2}} + \frac{1}{q_2^{1/2}}\left(\frac{q_1^2 F}{4q_2^2} - \frac{q_1}{2\sqrt{\pi} q_2^{3/2}}\right)\right]$$
$$= \sqrt{\pi}\left(\frac{1}{4q_2^{3/2}} + \frac{q_1^2}{8q_2^{5/2}}\right) F - \frac{q_1}{4q_2^2}$$
$$= \frac{\sqrt{\pi}(q_1^2 + 2q_2) F\left(\frac{q_1}{2\sqrt{q_2}}\right) - 2q_1 q_2^{1/2}}{8q_2^{5/2}} \qquad \text{(B3)}$$

Now we can replace q_1 and q_2 by their definitions mentioned below equation (29). Since the argument of F can also be written as $q_1/2\sqrt{q_2} = wq_1/2 \equiv X$, and because $q_1^2 + 2q_2 = 2(1+2X^2)/w^2$, and $2q_1 q_2^{1/2} = 4X/w^2$, we end up with eqation (32), i.e.

$$J = \frac{w^3}{4}\left[(1+2X^2)\sqrt{\pi} F(X) - 2X\right] \qquad \text{(B4)}$$

With the help of equation (A2), equation (B4) can be rewritten in a compact fashion as

$$J = \frac{\sqrt{\pi} w^3}{4}\frac{d}{dX}[XF(X)]. \qquad \text{(B5)}$$

Proof: Making use of the product rule and equation (A2)

$$J = \frac{\sqrt{\pi} w^3}{4}\left[F(X) + X\frac{dF(X)}{dX}\right]$$
$$= \frac{\sqrt{\pi} w^3}{4}\left[F(X) + 2X\left(XF(X) - \frac{1}{\sqrt{\pi}}\right)\right] \qquad \text{(B6)}$$

is obviously identical with (B4).

Appendix C: Asymptotic limits of the integral $J(X)$ and the reproduction factor $R(X)$

Here we investigate analytically the asymptotic limits of the integral $J(t)$ as given by eq (B4) or (B5), and the effective reproduction factor $R(t) = 2/b^3 J(t)$ according to eq (28) for the gamma-shaped serial interval distribution as function of the dimensionless time (31), now written in terms of Δ rather than x using definitions (30) and (31)

$$X = \frac{\Delta_c - \Delta}{w}, \qquad \Delta_c = \frac{bw^2}{2} \qquad \text{(C1)}$$

We investigate four limits: (**a**) very early times $\Delta \ll \Delta_c - w$, corresponding to very large positive values of the dimensionless time $X \gg 1$, (**b**) times $(\Delta_c - w) \ll \Delta \leq \Delta_c$ corresponding to small values of $0 \leq X \ll 1$. For times $\Delta \geq \Delta_c$ the dimensionless time $X = -\bar{X}$ is negative with positive $\bar{X} = (\Delta - \Delta_c)/w$. (**c**) times $\Delta_c \leq \Delta \ll \Delta_c + w$ corresponding to small values of $0 \leq \bar{X} \ll 1$, and (**d**) very late times $\Delta \gg \Delta_c + w$ corresponding to $\bar{X} \gg 1$. Consider each case in turn.

1. Case (a) $\Delta \ll \Delta_c - w$

As $X \gg 1$ we use the asymptotic expansion[5]

$$\sqrt{\pi} XF(X) \simeq 1 + \sum_{m=1}^{\infty} \frac{(-1)^m 1 \cdot 3 \cdots (2m-1)}{(2X^2)^m}$$
$$\simeq 1 - \frac{1}{2X^2} + \frac{3}{4X^4}, \qquad \text{(C2)}$$

implying

$$\sqrt{\pi}\frac{d}{dX}[XF(X)] \simeq \frac{1}{X^3} - \frac{3}{X^5} \qquad \text{(C3)}$$

Hence to lowest order in $X^{-1} \ll 1$ the function (B5) becomes

$$J(\Delta \ll \Delta_c - w) \simeq \frac{w^3}{4X^3} = \frac{w^6}{4(\Delta_c - \Delta)^3}, \qquad \text{(C4)}$$

corresponding according to equation (C1) to

$$R(\Delta \ll \Delta_c - w) \simeq \frac{8(\Delta_c - \Delta)^3}{b^3 w^6} = \left(\frac{\Delta_c - \Delta}{\Delta_c}\right)^3$$

$$= \left(1 - \frac{\Delta}{\Delta_c}\right)^3 = \left(1 - \frac{x}{x_c}\right)^3 \quad \text{(C5)}$$

Special case $\Delta = \Delta_0$. The inequality $\Delta \ll \Delta_c - w$ applies for the special case of $\Delta = \Delta_0$ as long as $w \gg 2/b = 9/2 = 4.5$ for the following reason. If $bw/2 \gg 1$, then $bw^2/2 = \Delta_c \gg w > w + \Delta_0$, because Δ_0 is negative. The analytical approximation (C5) then provides

$$R_0 = \left(1 - \frac{x_0}{x_c}\right)^3 = \left(1 + \frac{2\sqrt{\ln c_{\max}}}{bw}\right)^3, \quad \text{(C6)}$$

agreeing exactly with equation (34) that was derived using a different approach.

2. Case (b) $(\Delta_c - w) \ll \Delta \leq \Delta_c$

Here $0 \leq X \ll 1$ and we approximate

$$F(0 \leq X \ll 1) \simeq (1 + X^2)\left(1 - \frac{2}{\sqrt{\pi}}\int_0^X dy\,(1 - y^2)\right)$$
$$\simeq 1 - \frac{2X}{\sqrt{\pi}} + X^2 \quad \text{(C7)}$$

Consequently,

$$\frac{d}{dX}[XF(X)] \simeq 1 - \frac{4X}{\sqrt{\pi}} + 3X^2, \quad \text{(C8)}$$

so that to lowest order in $X \ll 1$

$$J(\Delta_c - w \ll \Delta \leq \Delta_c) \simeq \frac{w^3}{4}(\sqrt{\pi} - 4X) \quad \text{(C9)}$$

and

$$R(\Delta_c - w \ll \Delta \leq \Delta_c) \simeq \frac{w^4}{\Delta_c^3[\sqrt{\pi}w - 4(\Delta_c - \Delta)]} \quad \text{(C10)}$$

3. Case (c) $\Delta_c \leq \Delta \ll \Delta_c + w$

Here $0 \leq \bar{X} \ll 1$ using the short-hand notation $\bar{X} = -X$. According to equation (A3)

$$F(-\bar{X}) = 2e^{\bar{X}^2} - F(\bar{X}) \quad \text{(C11)}$$

and equation (B5) reads in terms of $\bar{X}$

$$J = \frac{\sqrt{\pi}w^3}{4}\frac{d}{d\bar{X}}[\bar{X}F(-\bar{X})]$$
$$= \frac{\sqrt{\pi}w^3}{4}\frac{d}{d\bar{X}}\left[2\bar{X}e^{\bar{X}^2} - \bar{X}F(\bar{X})\right] \quad \text{(C12)}$$

For $0 \leq \bar{X} \ll 1$ we use the asymptotic limit (C7) for

$$F(0 \leq \bar{X} \ll 1) \simeq 1 - \frac{2\bar{X}}{\sqrt{\pi}} + \bar{X}^2 \quad \text{(C13)}$$

yielding for

$$2\bar{X}e^{\bar{X}^2} - \bar{X}F(\bar{X}) \simeq \bar{X} + \frac{2}{\sqrt{\pi}}\bar{X}^2 + \bar{X}^3, \quad \text{(C14)}$$

so that

$$J(\Delta_c \leq \Delta \ll \Delta_c + w) \simeq \frac{\sqrt{\pi}w^3}{4}\left(1 + \frac{4\bar{X}}{\sqrt{\pi}}\right) \quad \text{(C15)}$$

and

$$R(\Delta_c \leq \Delta \ll \Delta_c + w) \simeq \frac{w^4}{\Delta_c^3[\sqrt{\pi}w + 4(\Delta - \Delta_c)]}, \quad \text{(C16)}$$

Equations (C15) - (C16) are identical to the former equations (C9) - (C10).

4. Case (d) $\Delta \gg \Delta_c + w$

Here $\bar{X} \gg 1$ with the positive $\bar{X} = -X$, so that equation (C12) still applies. For the present purpose we write it as

$$J = \frac{w^3}{4}\frac{d}{d\bar{X}}\left[2\sqrt{\pi}\bar{X}e^{\bar{X}^2} - \sqrt{\pi}\bar{X}F(\bar{X})\right], \quad \text{(C17)}$$

Since $\bar{X} \gg 1$ we use the approximation (C2) for F to obtain

$$J(\bar{X} \gg 1) \simeq \frac{w^3}{4}\frac{d}{d\bar{X}}\left[2\sqrt{\pi}\bar{X}e^{\bar{X}^2} - 1 + \frac{1}{2\bar{X}^2}\right] \quad \text{(C18)}$$

To leading order we thus find

$$J(\Delta \gg \Delta_c + w) \simeq \sqrt{\pi}w^3\bar{X}^2e^{\bar{X}^2}$$
$$= \sqrt{\pi}w(\Delta - \Delta_c)^2e^{(\frac{\Delta - \Delta_c}{\Delta_c})^2} \quad \text{(C19)}$$

and finally the very small reproduction factors

$$R(\Delta \gg \Delta_c + w) \simeq \frac{w^5e^{-(\frac{\Delta - \Delta_c}{w})^2}}{4\sqrt{\pi}\Delta_c^3(\Delta - \Delta_c)^2} \quad \text{(C20)}$$

Appendix D: Crossing the $R = 1$ line

1. Gamma-shaped $W(s)$

According to equation (33) $R(t)$ is unity when

$$\sqrt{\pi}\frac{d}{dX}[XF(X)] = -\frac{1}{x_c^3} \quad \text{(D1)}$$

As the right-hand side of this equation is a small positive number, we expect solutions of this equation for large values of X. Using the asymptotic expansion (C3) we obtain

$$\frac{1}{X^3} - \frac{3}{X^5} \simeq -\frac{1}{x_c^3} \quad \text{(D2)}$$

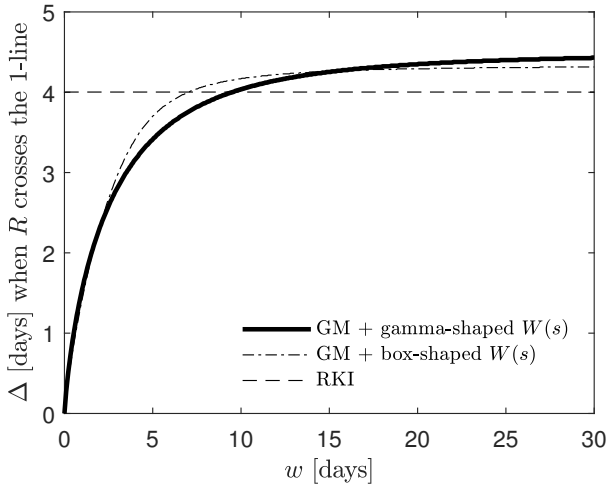

FIG. 8. The effective reproduction factor drops below unity Δ days after peak time. Shown is Δ as function of the peak width w for the GM with gamma-shaped (thick solid), box-shaped (dot-dashed) serial interval distribution, and the RKI factor.

with the solution

$$X \simeq -\frac{x_c}{(1+\frac{3}{x_c^2})^{1/3}} \simeq -x_c\left(1-\frac{1}{x_c^2}+\frac{2}{x_c^4}\right) = -x_c+\frac{1}{x_c}-\frac{2}{x_c^3}, \tag{D3}$$

where we used $(1+\epsilon)^{-1/3} = 1-(\epsilon/3)+(2\epsilon^2/9)$. With $X = (\Delta_c-\Delta)/w = -x_c-(\Delta/w)$ the solution (D3) corresponds to

$$\Delta = -\frac{w}{x_c}\left(1-\frac{2}{x_c^2}\right) = \frac{2}{b}\left[1-\frac{8}{(bw)^2}\right] \tag{D4}$$

To lowest order $\Delta = 2/b = 9/2 = 4.5$ days in agreement with Figs. 5 and 8.

2. Box-shaped $W(s)$

For the case of a box-shaped $W(s)$ we can do the corresponding calculation. We introduce $\eta = s_{\max}/w$ and $x = -\Delta/w$. $R(t)$ in equation (37) reaches unity when

$$\eta = \frac{\sqrt{\pi}}{2}e^{x^2}\left[\mathrm{erf}\,(x+\eta)-\mathrm{erf}\,(x)\right] \tag{D5}$$

With the integral representation of the error function we obtain

$$\eta = \int_0^\eta ds = \int_x^{x+\eta} dt\, e^{-(t^2-x^2)} \tag{D6}$$

Substituting on the right hand side $t = s+x$ leads to

$$\int_0^\eta ds\,[e^{-(s^2+2xs)}-1] = 0 \tag{D7}$$

We consider the limit where

$$\eta^2 + 2x\eta \ll 1, \tag{D8}$$

allowing us to approximate equation (D7) as

$$\begin{aligned} 0 &= \int_0^\eta ds\,[e^{-(s^2+2xs)}-1] \\ &\simeq -\int_0^\eta ds\,[s^2+2xs] \\ &= -\eta^2\,(x+\eta/3)\,, \end{aligned} \tag{D9}$$

yielding as solution

$$x = -\frac{\eta}{3} = -\frac{s_{\max}}{3w}, \tag{D10}$$

which fulfils the constraint (D8) for all values of $\eta \ll \sqrt{3}$. With $x = -\Delta/w$ the solution (D10) corresponds to $\Delta = s_{\max}/3$. Using $s_{\max} = 13$, this translates into $R(t) = 1$ at $\Delta = 13/3 \approx 4.33$, in agreement with Figs. 5 and 8.

1. Schüttler, J., Schlickeiser, R., Schlickeiser, F., Kröger, M., Covid-19 predictions using a Gauss model, based on data from April 2, medRxiv/2020/055830, DOI: 10.1101/2020.04.06.20055830 (2020, paper SSSK)
2. Schlickeiser, R., Schlickeiser, F., A Gaussian model for the time development of the Sars-Cov-2 corona pandemic disease. Predictions for Germany made on March 30, 2020, Physics, in press (2020), (medRxiv/2020/048942, DOI: 10.1101/2020.03.31.20048942 (2020))
3. Ciufolini, I., Paolozzi, A., Mathematical prediction of the time evolution of the COVID-19 pandemic in Italy by a Gauss error function and Monte Carlo simulations, Eur. Phys. J. Plus 135, 355 (2020).
4. Lixiang, L., Yang, Z., Dang, Z., Meng, C., Huang, J., Meng, H., Wang, D., Chen, G., Zhang, J., Peng, H., Shao, Y., Propagation analysis and prediction of the COVID-19, Infect. Disease Model. 5, 282-292 (2020).
5. Abramowitz, M., Stegun, I. A., Handbook of Mathematical Functions (NBS, Washington, 1972)
6. Schlickeiser, R., Cosmic magnetization: from spontaneously emitted aperiodic turbulent to ordered equipartition fields, Phys. Rev. Lett 109, 261101 (2012)
7. Flaxman, S., Mishra, S., Gandy, A., et al., Estimating the number of infections and the impact of non-pharmaceutical interventions on COVID-19 in 11 European countries. Imperial College London (30-03-2020) doi:

https://doi.org/10.25561/77731.

8. Scirea, J., Nadeaua, Vaughana, T., et al., Reproductive number of the COVID-19 epidemic in Switzerland with a focus on the Cantons of Basel-Stadt and Basel-Landschaft, https://ethz.ch/content/dam/ethz/special-interest/bsse/cevo/research/COVID-19/ScireEtAl-CHconfirmedCases.pdf (2020)
9. Fraser, C., Estimating individual and household reproduction numbers in an emerging epidemic, PLoS one **2**, e758 (2007).
10. Milligan, Gregg N., Barrett, Alan D. T., Vaccinology: an essential guide (Chichester, West Sussex: Wiley Blackwell), pp. 310 (2015)
11. Fraser, C., Donnelly, C. A., Cauchemez, S., Pandemic potential of a strain of influenza A (H1N1): Early findings, Science **324**, 1557-1561 (2009)